Supporting Information

Laser-Induced Graphene Layers and Electrodes Prevents Microbial Fouling and Exerts Antimicrobial Action

Swatantra P. Singh[1], Yilun Li[2], Avraham Be'er[1], Yoram Oren[1], James M. Tour[2*] and Christopher J. Arnusch[1*]

[1]*Department of Desalination and Water Treatment, Zuckerberg Institute for Water Research, The Jacob Blaustein Institutes for Desert Research, Ben-Gurion University of the Negev, Sede-Boqer Campus 84990, Israel*

[2]*Department of Chemistry, Department of Materials Science and NanoEngineering, Smalley-Curl Institute and NanoCarbon Center, Rice University, 6100 Main Street, Houston, Texas 77005, USA.*

***Corresponding author**: C. J. Arnusch, arnusch@bgu.ac.il and J M. Tour, tour@rice.edu

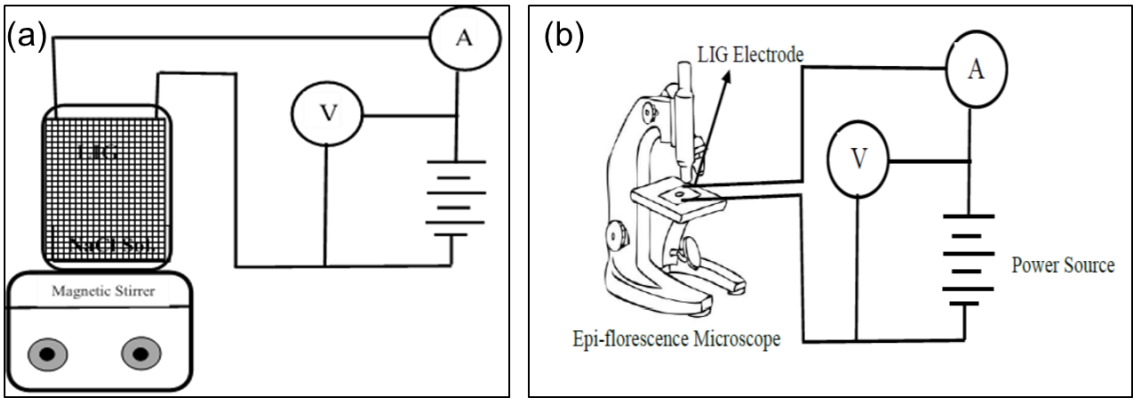

Figure S1: Antibacterial experiment with the LIG electrodes at different voltages (1.5, 2.0, 2.5 V). (a) Batch system; (b) Real time monitoring experiment under a microscope.

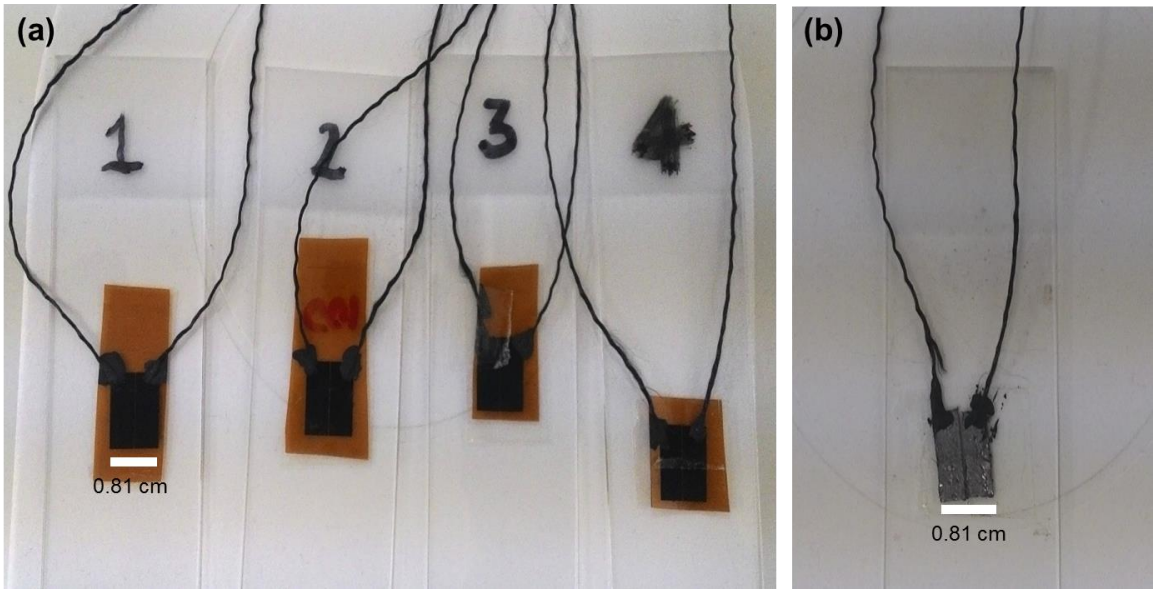

Figure S2: Electrodes for the real time monitoring of the *Pseudomonas aeruginosa* using epi-fluorescence microscopy; (a) LIG electrodes; (b) graphite paper electrode.

X-Ray Diffraction of the LIG:

The crystalline sizes of LIG along *c* axis (Lc) and domain size in the *a* axis (La) were calculated by using Equation 1 and Equation 2, respectively.

$$Lc = \frac{0.89\,\lambda}{B_{1/2}\,(2\theta)\,Cos\theta} \quad (1)$$

$$La = \frac{1.84\,\lambda}{B_{1/2}\,(2\theta)\,Cos\theta} \quad (2)$$

Where $B_{1/2}\,(2\theta)$ (in radian unit) is the full width and half maximum of peaks, and λ is X-ray wavelength (λ=1.54Å). Lc and La are calculated to be 1.8 and 5.8 nm, respectively.

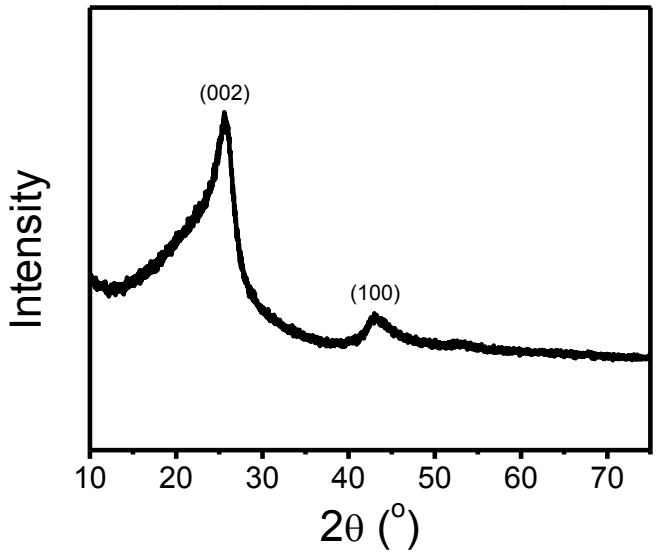

Figure S3: XRD of the powder LIG.

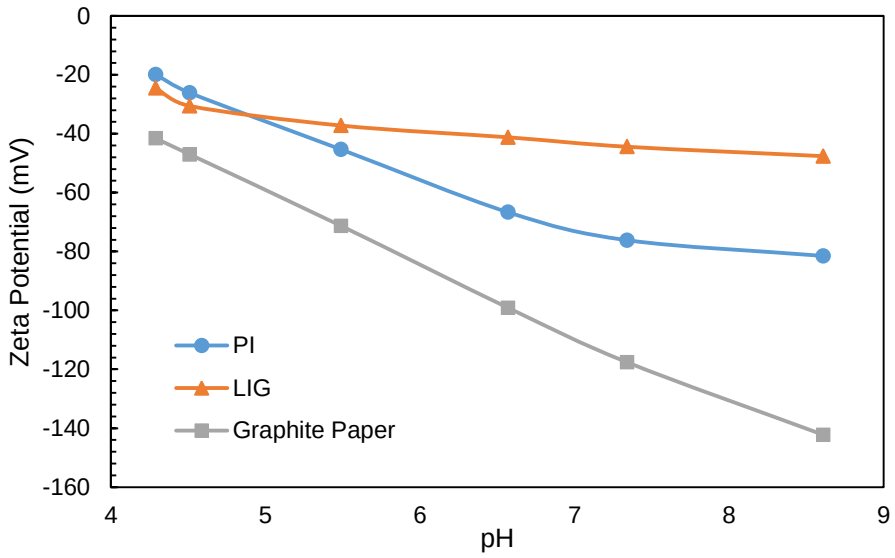

Figure S4: Zeta potential of different surfaces at different pH.

Figure S5: Contact angles for the (a) LIG film on PI , (b) PI, and (c) graphite paper are measured to be 45.3 ± 3.8°, 74.5 ± 3.3° and 61.3 ± 6.6°, respectively.

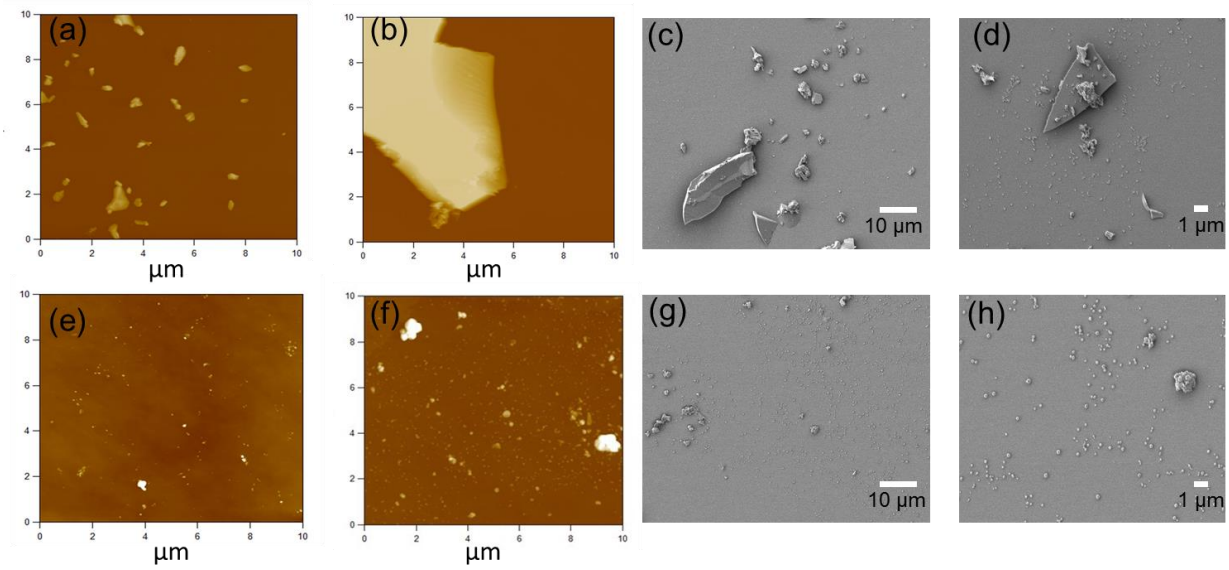

Figure S6: Atomic force microscopy (AFM) and scanning electron microscopy (SEM) images for powder LIG; (a & b) AFM images for P-LIG-B; (c & d) SEM images for P-LIG-B; (e & f) AFM images for P-LIG-S; (g & h) SEM images for P-LIG-S.

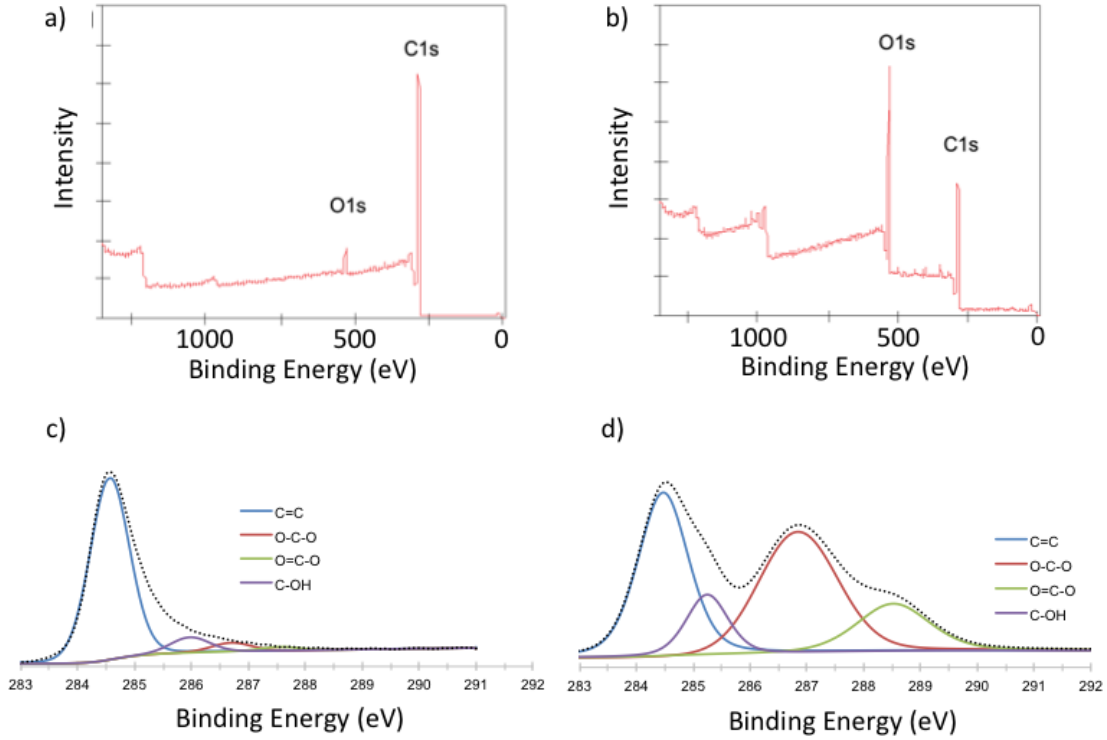

Figure S7: X-ray photoelectron spectra of LIG powders; (a, c) Before oxidation; (b, d) after oxidation.

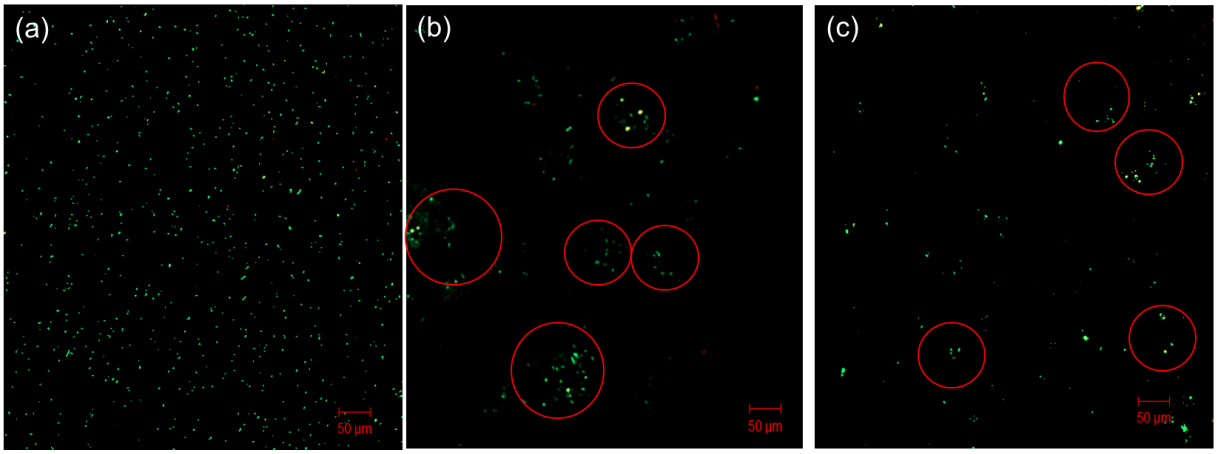

Figure S8: Representative epi-fluorescence picture of *Pseudomonas aeruginosa* in LIG suspension (Green: live cells, Red: dead cells); (a) Bacterial suspension with no LIG; (b) Bacterial suspension with P-LIG-B, red circles are showing LIG powder and bacterial cells aggregates; (c) Bacterial suspension with P-LIG-S.

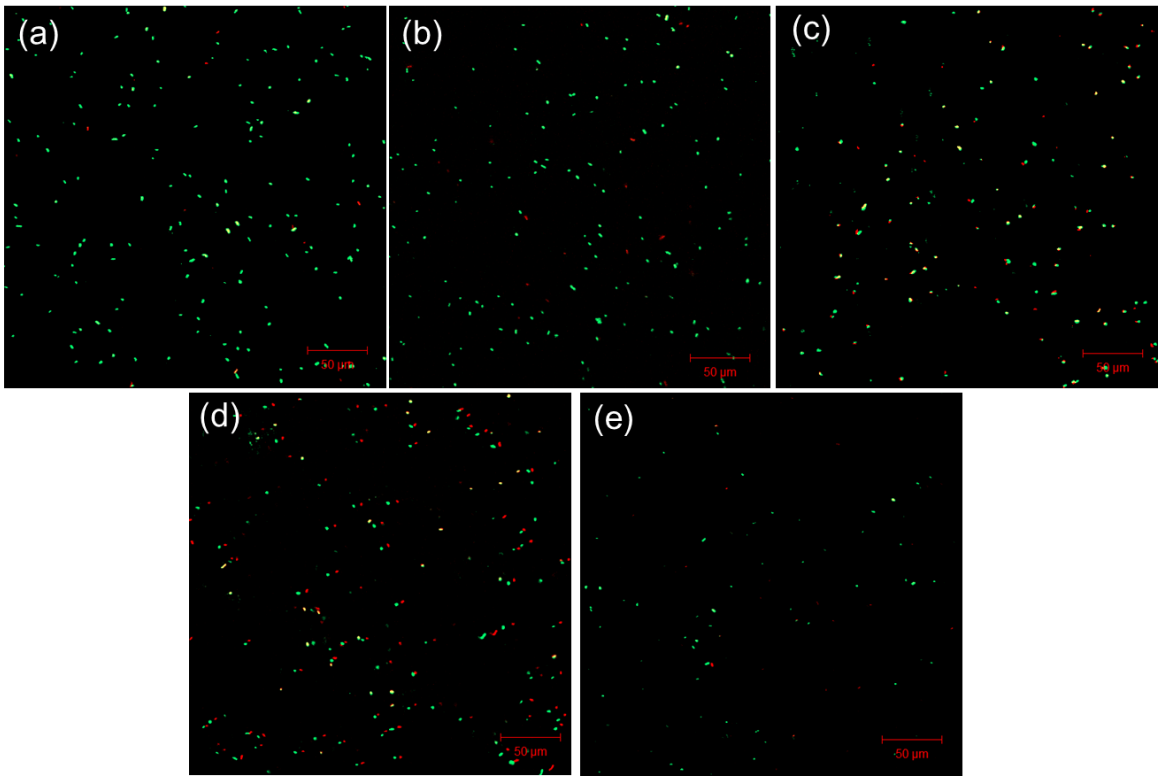

Figure S9: Representative epi-fluorescence picture of *Pseudomonas aeruginosa* on different surfaces (Green: live cells, Red: dead cells); (a) Cells on mixed cellulose filter; (b) Cells on mixed cellulose filter coated with P-LIG-B; (c) Cells on mixed cellulose filter coated with P-LIG-S; (d) Cells on mixed cellulose filter coated with P-LIG-SO; (e) Cells on 2% LIG film.

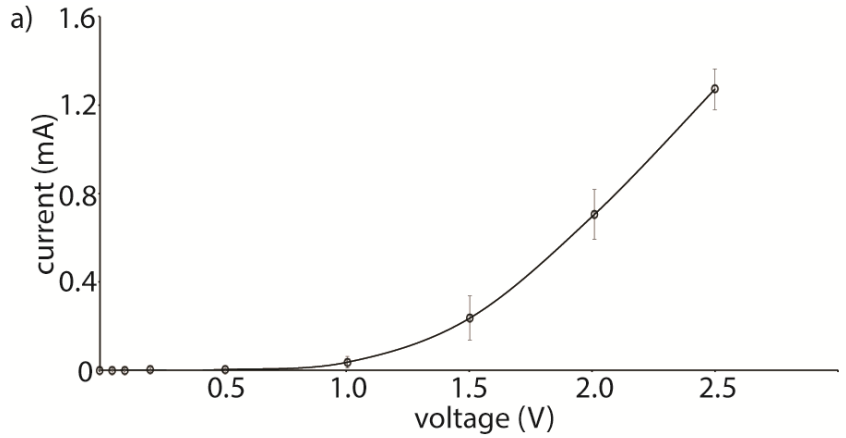

Figure S10: Current voltage relationship with the LIG electrodes in antibacterial batch experiments.

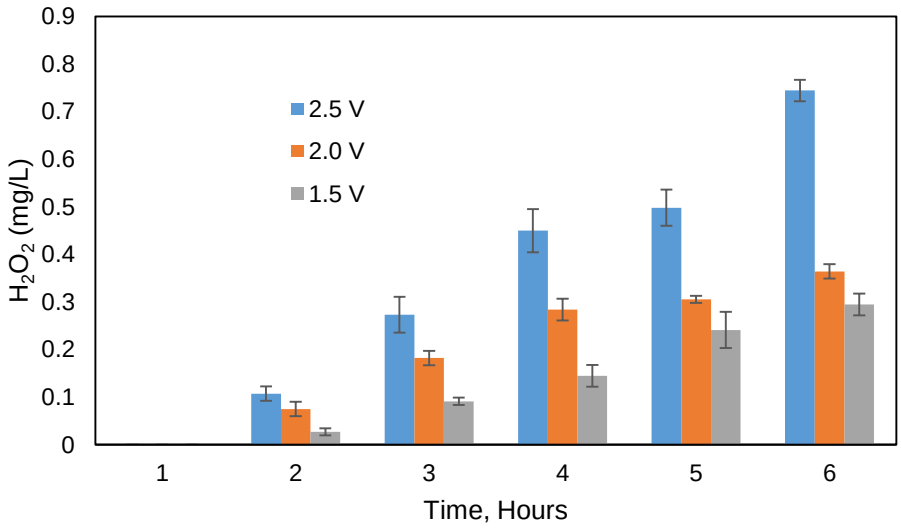

Figure S11: H_2O_2 generation in bulk solution with low bacteria load.

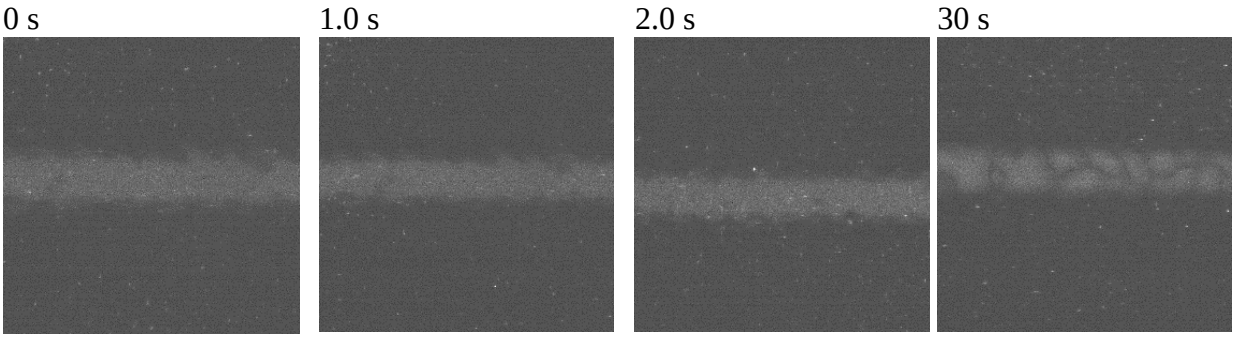

Figure S12: Real time bacterial population observation under epi-florescent microscopy at 1.1 V. In each image, a 100 µm channel separates the anode (top), from the cathode (bottom).

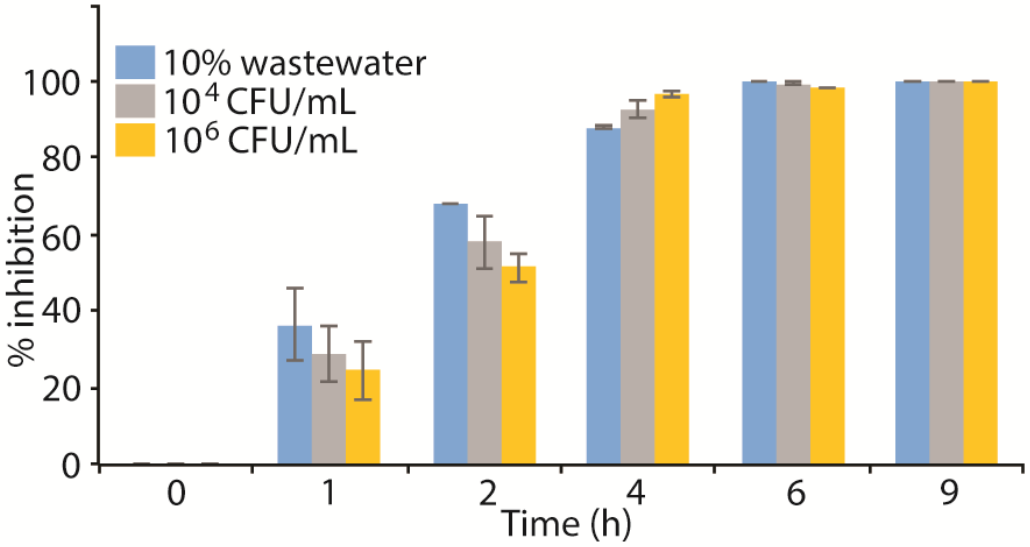

Figure S13: Inhibition of microbial growth expressed as % inhibition using various secondary treated wastewater solutions at 2.5 V.

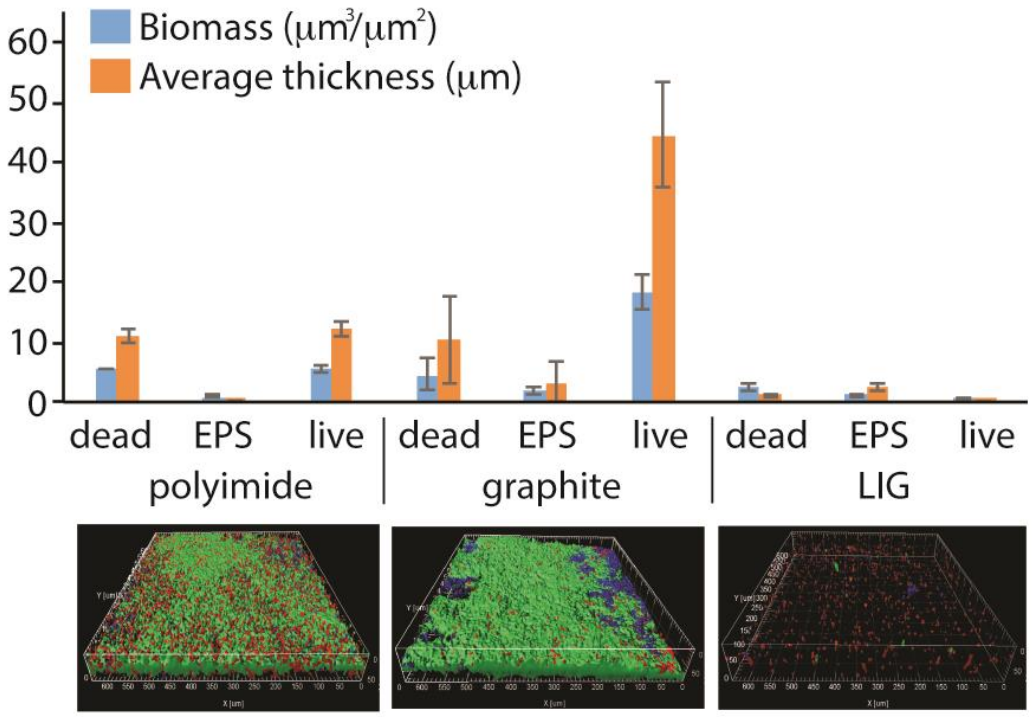

Figure S14: Biofilm growth on the polyimide, graphite, and LIG surfaces with using secondary treated wastewater showing biomass and average thickness. Representative IMARIS software images for polyimide; graphite; and LIG are seen. Green, red, and blue represents live bacteria, dead bacteria, and EPS, respectively.

Table S1: H_2O_2 (1.0 mg/L) is added to a solution with low bacterial concentration, and the bacterial viability and the H_2O_2 is monitored over time. The control is the solution with no H_2O_2 added.

Low Loading		
Time (h)	Measured H_2O_2 Conc. (mg/L)	% Killing relative to control
0	1.07	0.00
1	0.92	6.26
2	0.84	4.09
4	0.75	0.77
6	0.69	4.26
9	0.49	4.63

Table S2: H_2O_2 (1.0 mg/L) is added to a solution with high bacterial concentration, and the bacterial viability and the H_2O_2 is monitored over time. The control is the solution with no H_2O_2 added.

High Loading		
Time (h)	Measured H_2O_2 Conc. (mg/L)	% Killing relative to control
0	1.09	0.00
1	0.26	5.45
2	0.18	4.56
4	0.13	7.44
6	0.00	4.12
9	0.00	1.09

Table S3: Change in current with voltage in microscope electrodes.

Microscope Electrodes		
Voltage (V)	LIG Electrode Current (μA)	Graphite Paper Current (μA)
0	0	0
0.1	3.2	0.1
0.5	28.5	0.6
1	67.2	4.2
1.5	105.6	42.5
2	152.3	86.5
2.5	203.8	110.4

Table S4: Secondary treated wastewater composition.

	Value (ppm)
BOD_5	55
TOC	122
Nitrogen	20
Phosphate	15